

# Use of Nanoparticles for Improving the Foaming Behaviors of Linear PP

W. G. Zheng,<sup>1,2</sup> Y. H. Lee,<sup>3</sup> C. B. Park<sup>2</sup>

<sup>1</sup>Ningbo Key Laboratory of Polymer Materials, Division of Polymers and Composites, Ningbo Institute of Material Technology & Engineering, Chinese Academy of Sciences, Ningbo 315201, China

<sup>2</sup>Microcellular Plastics Manufacturing Laboratory, Department of Mechanical and Industrial Engineering, University of Toronto, Toronto, Ontario M5S 3G8, Canada

<sup>3</sup>Centre for Biocomposites and Biomaterials Processing, Faculty of Forestry, University of Toronto, Ontario M5S 3B3, Canada

Received 7 April 2009; accepted 5 February 2010

DOI 10.1002/app.32253

Published online 27 April 2010 in Wiley InterScience (www.interscience.wiley.com).

**ABSTRACT:** This research presents the foaming behaviors of linear polypropylene (PP) and PP/clay nanocomposites blown with supercritical CO<sub>2</sub>. The cell nucleation and expansion behaviors of the linear PP and PP-based nanocomposites at various clay contents during extrusion foaming are studied. The experimental results indicate that the nano-particles have a posi-

tive impact on improving the cell morphology, the cell density and the expansion ratio of the linear PP foams. © 2010 Wiley Periodicals, Inc. *J Appl Polym Sci* 117: 2972–2979, 2010

**Key words:** polypropylene; extrusion foaming; physical blow agent; nanocomposite; foam

## INTRODUCTION

Polymeric foams are materials with a distinct cellular structure that resulted from the expansion of a blowing agent, usually a volatile gas or liquid, which was dissolved in polymers. These foams have wide applications in insulation and packaging, as well as in the automotive and construction industries because of their excellent properties; they are light-weight and exhibit a high strength-to-weight ratio, superior insulating qualities, and excellent energy absorption.<sup>1</sup> The foaming process is complicated and is governed by interactions between polymers, blowing agents, and nucleating agents under specific processing conditions.<sup>1–4</sup> Fundamental matters of solubility and diffusivity have been systematically investigated as they are pertinent to both academic and industrial interests.<sup>1–4</sup> It has long been expected that PP foams would be adopted as a substitute for other thermoplastic foams in industrial applications because of their first-rate functional properties and low material cost. However, limited researches have been conducted on the production of PP foams because of their weak melt strength and

melt elasticity, which compromise their production and thus make it difficult to study PP foams in relation to other available plastics.<sup>5</sup> If the melt strength is too weak the cell walls separating the bubbles will not be strong enough to bear any extensional force, and these bubbles are already susceptible to coalescence and rupture during foam processing. As a result, the foamed PP products usually have high open-cell content and are not good for practical applications.

A number of studies have inquired into means to compensate for PP's weak melt strength. Commercial branched PP, for example, was developed for producing good PP foams. The branched PP was found to be very satisfactory for manufacturing PP foamed products,<sup>6,7</sup> as branched PP has a high melt strength that suppresses bubble coalescence.<sup>7</sup> However, the cost of branched PP is much higher than that of linear PP, and use of branched PP is therefore often avoided. Park and Cheung<sup>8</sup> conducted a comparison between the effects of branched PP and linear PP on cell nucleation and growth. It was found that linear PP demonstrated a higher nuclei density than that in branched PP. However, poor foam morphology was obtained for linear PP because of severe cell coalescence, which caused the opening of most cells and yielded interconnections within the linear PP foams. The branched PP, on the other hand, produced a better foam structure because of its capacity to enhance bubble stability. Only when the extruded foams were quenched

Correspondence to: C. B. Park (park@mie.utoronto.ca).

Contract grant sponsors: AUTO21, Consortium for Cellular and Micro-Cellular Plastics (CCMCP).

using water to minimize bubble coalescence, the final cell density for the linear PP was higher than that for the branched PP. It appears that the key issue for preparing good linear PP foams is to suppress the cell coalescence that results from the weak melt strength of linear PP.

The addition of nanoclay to polymers to produce nanocomposites has been widely utilized in an attempt to improve the mechanical, thermal, and gas barrier properties of polymers.<sup>9–12</sup> The nanoclay particles have a platelet-like geometry and are composed of layers that are almost 1 nm in thickness. The high aspect ratio and large surface area of nanoclay particles offer the potential for good reinforcing efficiency and improved dimensional and thermal stability. The PP/clay nanocomposite configuration is a widely investigated one amongst polymer nanocomposites. The automotive industry, for instance, has been employing this combination increasingly. General Motors has taken the lead in putting nanocomposites on the road. GM launched the first commercial use of TPO nanocomposites in auto exteriors; the step assist on the 2002 GMC Safari and Chevrolet Astro van was made from this material. The part also appears on 2003 and 2004 models. More recently, a PP/nanoclay composite appeared on the body side-molding of GM's highest volume car, the 2004 Chevrolet Impala as well as in the centre bridge, sail panel, and box-rail protector of the 2005 GM Hummer H2 SUT.<sup>13</sup> The increasing use of polymer nanocomposites in industries is based on the excellent mechanical properties of polymer nanocomposites even with lower filler loadings. The flexural modulus of PP/clay nanocomposites with 5 wt % clay loading is higher than that of PP/talc composites with 20 wt % loading. The mechanical properties of the PP/clay nanocomposites are significantly dependant upon the dispersion and exfoliation of the nanoparticles in the nanocomposites, which is greatly affected by the coupling agent, the characteristic properties of the PP, and the processing conditions.<sup>9</sup> The better the clay dispersion and exfoliation in polymer/clay nanocomposites are the higher the mechanical properties of final nanocomposites.<sup>9</sup>

Recently, nanoclay particles have also been used in the polymer nanocomposite foaming process, serving as efficient nucleating agents that help to decrease the foam cell size and increase the foam cell density.<sup>14–18</sup> Previously, micrometer-size fillers were employed to this end.<sup>19–21</sup> However, what distinguishes clay nanoparticles from traditional microfillers is that the role of nanoparticles in polymer foaming may not be simply limited to cell nucleation, but may also encompass significant functions that promote polymer foamability and affect foam morphologies. In our previous paper,<sup>22</sup> we found that the addition of small amounts of nanoparticles can

greatly improve the morphologies of polymers with low melt viscosities and melt strengths. It is believed that well-dispersed nanoparticles in polymer nanocomposites will change substantially both the rheological behaviors of polymers and the foaming results.

In this study, a small amount of clay was compounded with PP to form PP-based nanocomposites. PP and its nanocomposites of varying clay contents were foamed in extrusion using CO<sub>2</sub> as a blowing agent. The effect of the physical blowing agent (CO<sub>2</sub>) on the intercalation of the clay particles is reported. It was determined that the severe cell coalescence that occurs with linear PP can be suppressed when a small amount of clay particles is added.

## EXPERIMENTAL

### Materials

Linear PP, HE351 with MFI of 12 g/10 min at 230°C/2.16 Kg, was provided by Borealis GmbH of Austria. PP-MAH, Fusabond MD511D with MFI of 24 g/10 min at 190°C/2.16 Kg was supplied by Dupont Canada. Cloisite<sup>®</sup> 20A (herein termed "clay"), manufactured by Southern Clay Products, is a natural montmorillonite modified with dimethyl dehydrogenated tallow quaternary ammonium chloride. The physical blowing agent, CO<sub>2</sub> (99% purity), was made available by BOC Canada.

### Nanocomposite preparation and characterization

All polymers were vacuum dried at 80°C for 8 h before use. The linear PP matrix (LPP) was dry-blended using the same weight proportions of PP with PP-MAH. An LPP/clay premix was prepared by dry-blending the clay with LPP; the premix was subsequently melt-extruded using a twin-screw extruder at a temperature of 200°C. The clay contents prepared for the masterbatch nanocomposites were 1 and 5 wt %, respectively. LPP/clay nanocomposites with clay content of 0.2 and 0.5 wt % were prepared by diluting PP/clay 1 wt % with LPP. The nanocomposite pellets were hot-pressed at 200°C to make a film for X-Ray Diffraction (XRD) analysis and transmission electron microscopy (TEM) analysis to enable an investigation of the clay dispersion and exfoliation. XRD spectra were collected on a Siemens D5000 diffractometer equipped with a Kevex solid-state detector that uses a Cu K $\alpha$  radiation source with a wavelength of 1.54Å. Measurement was performed at 50 kV and 35 mA. The data were recorded in the reflection mode at range of  $2\Theta = 1.5\text{--}10^\circ$  using STEP scan mode. The step size was 0.02 degrees and the counting time was 2.0 s per step. For TEM analysis, the sample was microtomed to an ultrathin section (70 nm in thickness) using an ultracryo

microtome with a diamond knife. The images were obtained from an FEI Technai 20 (Phillips) apparatus that uses an accelerating voltage of 200 kV. The foaming samples were also hot-pressed at 200°C to create a film for XRD and TEM analysis, which enabled the study of the effects of the physical blowing agent on clay exfoliation in PP/clay nanocomposites that take place once the foaming experiment has run to completion.

### Extrusion foaming experiments and characterization

The extrusion foaming system used in the experiment is described in references.<sup>20–22</sup> A filamentary die with L/D 0.300"/0.018" was used for the foaming experiments. The gas content injected into the barrel, which was fixed at 5 wt % CO<sub>2</sub> throughout the experiment, was accurately adjusted and regulated by controlling both the CO<sub>2</sub> flow rate of at the syringe pump and the flow rate of the materials once they had passed through the die. The die temperature here was equivalent to the temperature of the die and the heat exchanger. The foaming samples were collected and examined by SEM to evaluate the foam cell morphology and obtain a density measurement for the volume expansion ratio and/or foam void fraction. A Jeol JSM 6060 SEM was used to investigate the foam cell morphology. The foam samples were freeze-fractured in liquid nitrogen to expose their cellular morphology, and then the fracture surface was sputter-coated with gold before observation. Cell size, volume expansion ratio (VER), and cell population density are the three key parameters for characterizing the foam structure.<sup>1,22</sup> These parameters can be derived from the SEM photos combined with the foam density data. Detailed information regarding the SEM characterization of foams can be found in our previous papers.<sup>22</sup>

## RESULTS AND DISCUSSION

### Structure of LPP/clay nanocomposites

The nanoclay used in this study is a commercial clay product, Cloisite® 20A (herein termed "clay"), which is a natural montmorillonite modified with dimethyl dehydrogenated tallow quaternary ammonium chloride. It is suitable for polyolefin nanocomposites when it is compounded directly with PP using a twin-screw extruder. Figure 1 is the XRD spectra of nanocomposite-clay combinations; it shows the typical (001) peak changes of clay in the raw clay and in the LPP/clay nanocomposites before and after the foaming experiments. Clay 20A had an apparent (001) peak at  $2\theta = 3.5^\circ$ , which corresponded to the layer spacing of 2.5 nm. After compounding the clay

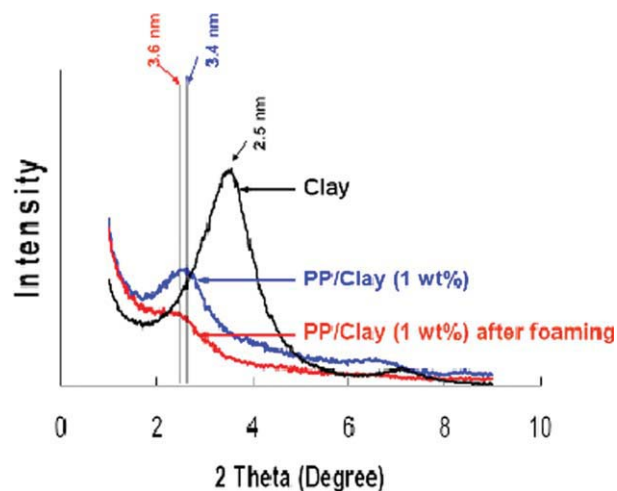


**Figure 1** XRD spectra of clay 20A and PP/clay (1 wt %) nanocomposites before and after foaming. [Color figure can be viewed in the online issue, which is available at [www.interscience.wiley.com](http://www.interscience.wiley.com).]

with LPP, the clay (001) peak shifted to  $2\theta = 2.6^\circ$ , which corresponded to the layer spacing of 3.4 nm in the PP nanocomposites. The increase in the layer spacing in the clay structure revealed that some polymer molecular chains were intercalated with the layer structure of the clay particles. The intensity decrease of the clay (001) peak in the PP/clay nanocomposites was because of the delamination of the clay stacks that occurred during melt processing. The results indicate that intercalated PP/clay nanocomposite can be prepared using a twin-screw extruder, which is consistent with the findings documented in several other studies.<sup>9–12</sup> The result of note in this particular experiment is that the clay (001) peak can be shifted further to  $2\theta = 2.4^\circ$ , which corresponds to a layer spacing of 3.6 nm in the PP nanocomposites after the foaming experiments had run to completion. The intensity of the clay's (001) peak of in the PP/clay nanocomposites after foaming with CO<sub>2</sub> was greatly reduced, which indicated that the intercalation and exfoliation of the clay particles were improved significantly by the foaming process. Figure 2 is the TEM images of the LPP/clay nanocomposites with 1 wt % clay, before and after the foaming experiments, which shows the better intercalation and exfoliation of the clay particles in LPP/clay nanocomposites after foaming.

The improved clay intercalation and exfoliation in the LPP/clay nanocomposites during the foaming process may have been due to following: (1) the lower viscosity because of supercritical CO<sub>2</sub> may have benefited the exfoliation process of the clay particles; and (2) the supercritical CO<sub>2</sub>, which would have interacted with the PP-MAH and the clay particles, thereby promoting the exfoliation of the clay particles in the PP/clay nanocomposites because of

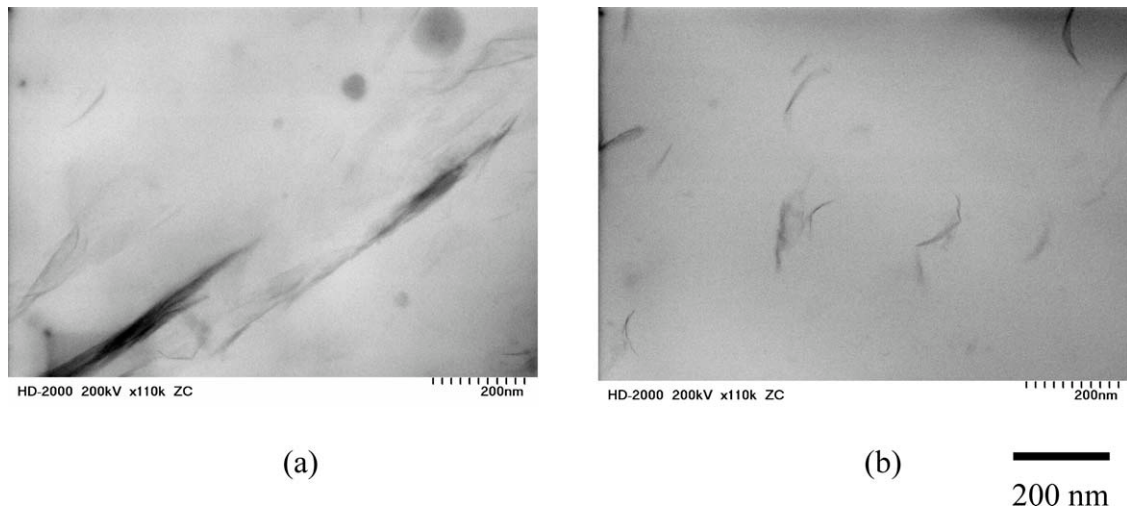


**Figure 2** TEM images of LPP/clay (1 wt %) nanocomposites; (a) before foaming, and (b) after foaming. The scale bar is 200 nm.

the “expansion effect” from the rapid pressure release during foam processing. The details of which mechanism dominates the promotion of clay intercalation and exfoliation regarding the effects of supercritical  $\text{CO}_2$  on the exfoliation of clay in PP/clay nanocomposites are still under investigation. A full understanding of the role of supercritical  $\text{CO}_2$  in clay exfoliation in PP/clay nanocomposites would enable

the development of more effective ways of exfoliating the clay particles in PP/clay nanocomposites.

#### PP and nanocomposite foams

The polymer and nanocomposite materials were foamed in extrusion with 5 wt %  $\text{CO}_2$  using a filament die. Figure 3 shows SEM micrographs of LPP

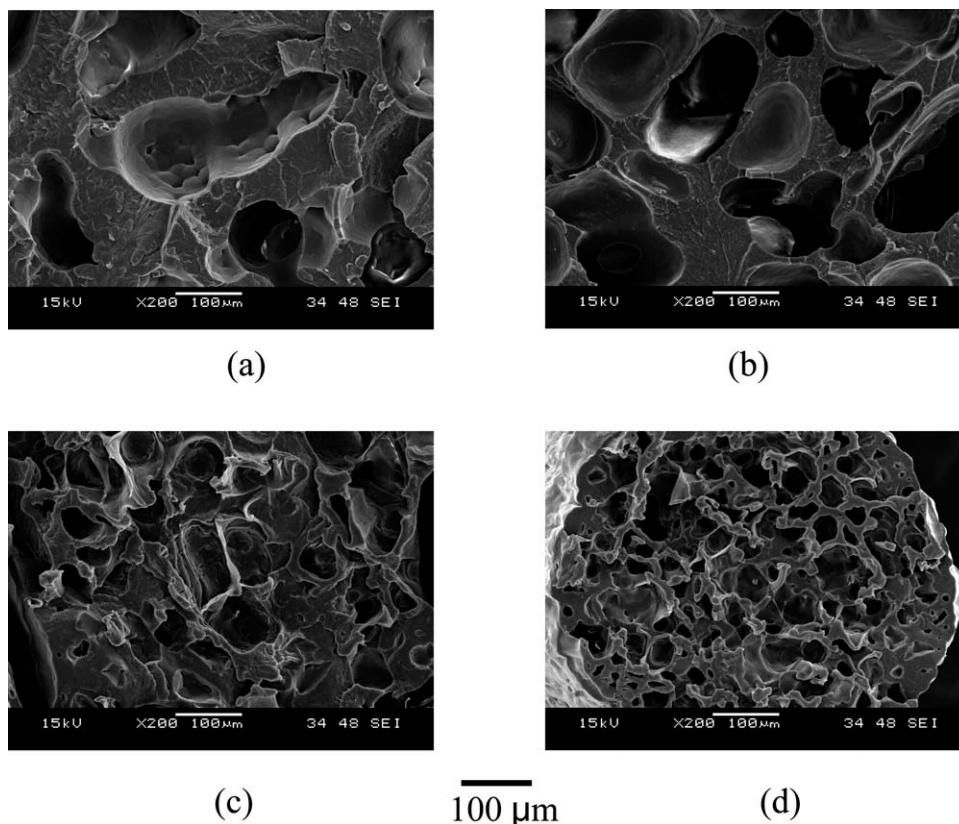


**Figure 3** SEM images of LPP foam at different die temperature: (a) 160°C; (b) 150°C; (c) 140°C; and (d) 135°C. The scale bar is 100  $\mu\text{m}$ .  $\text{CO}_2$  content injected to barrel is fixed to 5 wt %.

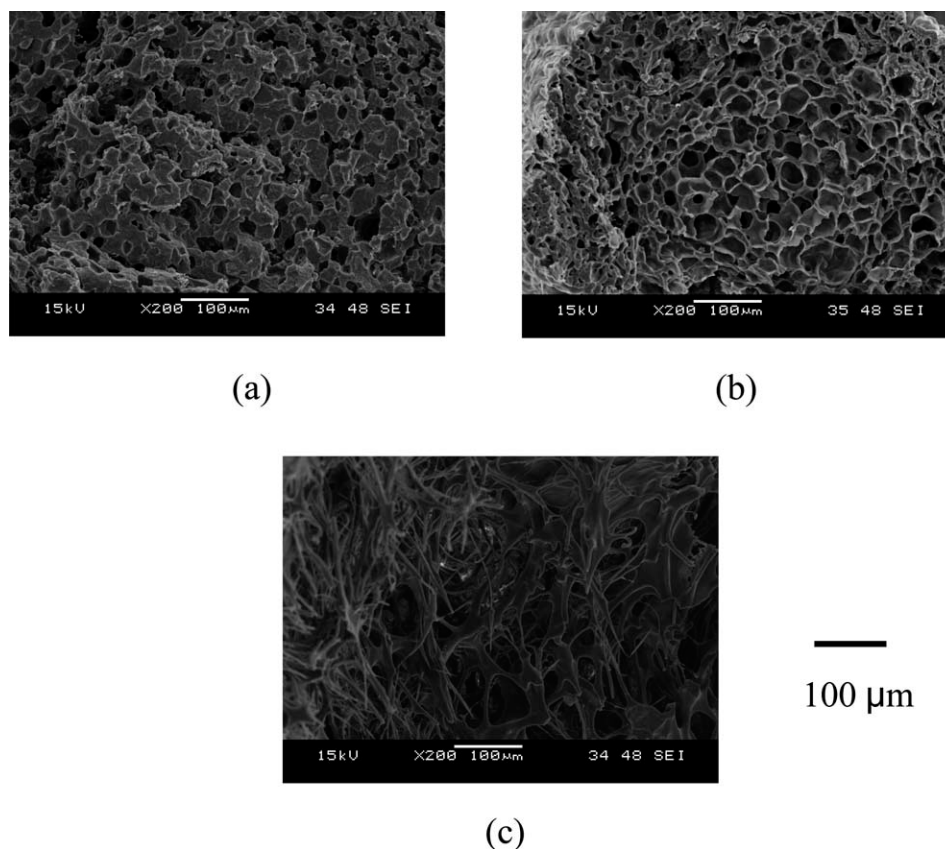


**Figure 4** SEM images of LPP/clay (1 wt %) nanocomposite foams at different die temperature: (a) 160°C; (b) 150°C; and (c) 145°C. The scale bar is 100  $\mu\text{m}$ .  $\text{CO}_2$  content injected to barrel is fixed to 5 wt %.

foam cell morphology at different die temperatures. Poor foam morphology was recorded for LPP because of the advent of severe cell coalescence, which caused most cells to open and form interconnections with one another in the linear PP foams. The result was similar to that reported in Park and Cheung paper.<sup>8</sup> The decrease in the die temperature only slightly improved the foam morphology of LPP foams.

The SEM micrographs in Figure 4 illustrate the foam cell morphology of LPP/clay (1 wt %) nanocomposite at different die temperatures. The foam morphology of LPP's is typically poor, but will undergo substantial improvements when 1 wt % clay is added to LPP/clay nanocomposite foams. Many viable closed cells were found in the LPP/clay nanocomposites, especially at a die temperature of 150°C. However, the die temperature cannot dip below 145°C in this process; below this temperature, LPP/clay (1 wt %) nanocomposites cannot be foamed because the clay particles will be subject to stiffening. The results indicate that the addition of a small amount of clay particles to LPP does in fact suppress cell coalescence, thus confirming that this process leads to the effective manufacturing of good LPP foams. To investigate the effect of clay content

on the foaming behaviors of LPP/clay nanocomposites, different clay contents were designed to fulfill this objective.

Figure 5 shows the effects of clay content on the foam morphology of LPP/clay nanocomposite foams at a die temperature of 150°C. When the clay content was lower (0.2 wt %), it appears that the foam morphology of nanocomposite foams is improved a little compared with the LPP foam. However, it should be noted that the lower clay content does not completely suppress cell coalescence. In cases where the clay content was 0.5 and 1 wt %, the SEM micrographs reveal completely closed cells in LPP, which means that cell coalescence was suppressed. However, even while results indicated that cell coalescence in LPP could be completely suppressed when the clay content was higher (5 wt %), the quality of foam products developed by this route may be compromised by the higher clay content, which can cause a stiffening of the polymer molecular chain, hinder cell growth during the foaming process, and also lead to increases in overall foam density.

Figure 6 demonstrates the effects of die temperature on the foam volume expansion ratio of LPP and LPP/clay nanocomposites at different clay contents. It was found that the foam volume expansion ratio

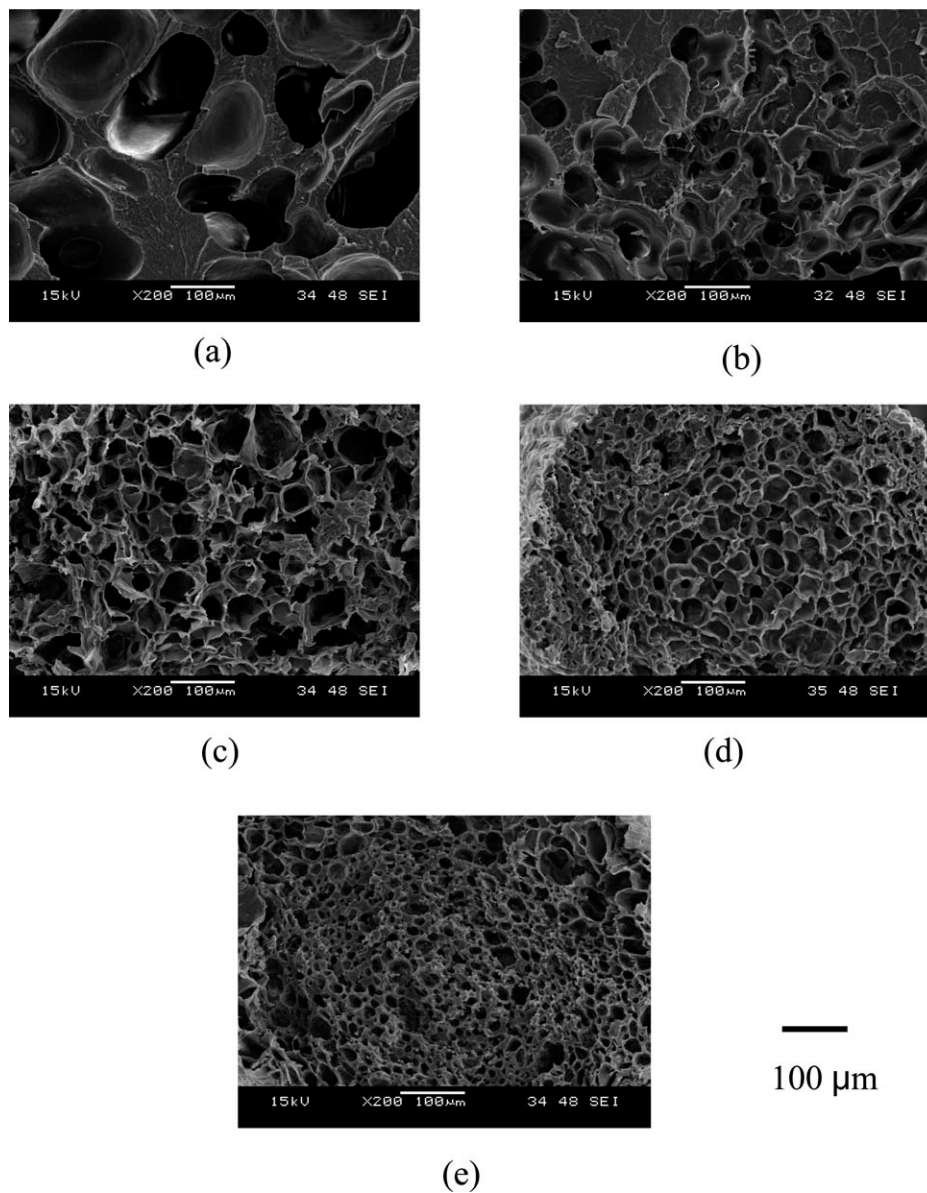


**Figure 5** SEM images of LPP/clay nanocomposite foams with different clay content: (a) 0 wt %; (b) 0.2 wt %; (c) 0.5 wt %; (d) 1.0 wt %; and (e) 5.0 wt %. The scale bar is 100  $\mu\text{m}$ .  $\text{CO}_2$  content injected to barrel is fixed to 5 wt %.

generally increased as the die temperature decreased. LPP foam had the lowest volume expansion ratio, which may have been due to the low viscosity and weak melt strength of LPP. Gas rapidly escapes from the hot skin of LPP foams during the foaming process. On the other hand, LPP/clay nanocomposites showed higher volume expansion ratios. The reason for this is possibly due to the barrier role played by well-dispersed clay particles, which help to retain gas for cell growth and thus lead to an increase in the volume expansion ratio. Similar results can be found in our earlier paper on the foaming of PA6/clay nanocomposites.<sup>22</sup>

Figure 7 depicts the effects of clay content on the foam volume expansion ratio of LPP and LPP/clay nanocomposites at a die temperature of 150°C and

145°C. It was determined that the optimum clay contents were 0.5 and 1 wt %; at these levels, higher foam volume expansion ratio (around 5) were promoted in LPP/clay nanocomposites. As discussed in the previous section, a lower clay content (0.2 wt %) does not completely suppress cell coalescence in LPP, while a higher clay content (5 wt %) causes stiffening in the polymer molecular chain that is crucial for cell growth; in both cases, the foam volume expansion ratio is reduced.

Figure 8 illustrates the effects of die temperature on the foam cell density of LPP and LPP/clay nanocomposites at different clay contents. It was found that the cell density of LPP foams increased when the die temperature was decreased, as the reduced die temperature slightly suppresses cell coalescence

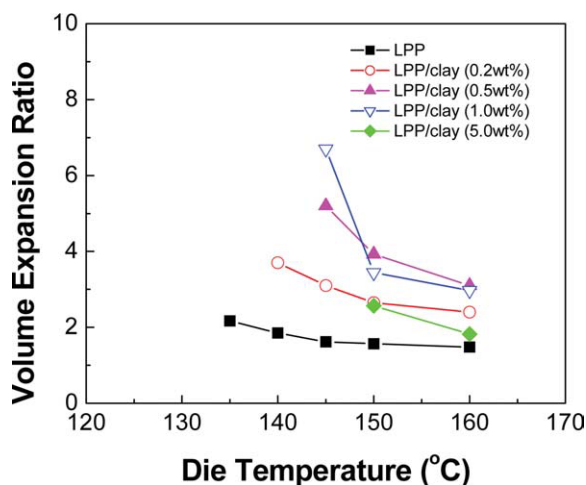


**Figure 6** Effect of die temperature on foam volume expansion ratio of LPP and LPP/clay nanocomposite foams with different clay content. [Color figure can be viewed in the online issue, which is available at [www.interscience.wiley.com](http://www.interscience.wiley.com).]

in LPP foams. When the clay content was lower (0.2 wt %), the foams also showed similar die temperature dependence behaviors even though they exhibited a higher cell density than LPP foams. When the clay content was above 0.5 wt %, the nanocomposite foams did not show any die temperature dependence, which indicated that the cell coalescence in LPP foams could be completely suppressed and all cell nuclei can be kept for cell growth to reach stable cell density.

Figure 9 shows the effects of clay content on the foam cell density of LPP and LPP/clay nanocomposites at a die temperature of 150°C. It was ascertained that the foam cell density of LPP ( $2 \times 10^7$  cells/cm<sup>3</sup>) could be increased significantly (up to  $2 \times 10^8$  cells/cm<sup>3</sup>) by the addition of nanoparticles,

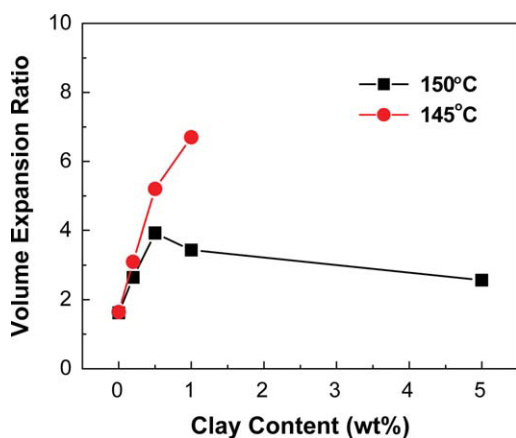


**Figure 7** Effect of clay content on foam volume expansion ratio of LPP/clay nanocomposite foams at die temperature of 150 and 145°C. [Color figure can be viewed in the online issue, which is available at [www.interscience.wiley.com](http://www.interscience.wiley.com).]

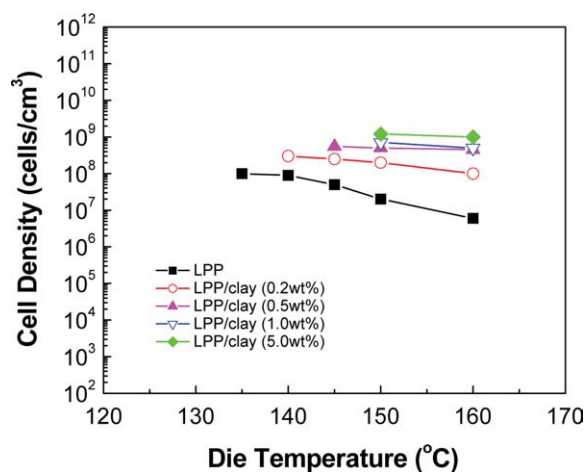


**Figure 8** Effect of die temperature on foam cell density of LPP and LPP/clay nanocomposite foams with different clay content. [Color figure can be viewed in the online issue, which is available at [www.interscience.wiley.com](http://www.interscience.wiley.com).]

even when the clay content was not high (0.2 wt %). The foam cell density of LPP/clay (5 wt %) reached  $1.3 \times 10^9$  cells/cm<sup>3</sup>. Here the experimental results confirmed the suppressive effect of clay particles on the severe cell coalescence that occurs in LPP, which in turn increases the foam volume expansion ratio and cell density of LPP/clay nanocomposite foams.

## CONCLUSIONS

This study investigated both the effects of a physical blow agent (CO<sub>2</sub>) on the clay exfoliation that takes place in the foaming processing of LPP/clay nanocomposites, as well as the effects of clay on foaming behaviors in LPP and its nanocomposites. The experimental research leads to the following conclusions: (1) supercritical CO<sub>2</sub> is helpful for expanding further the layer spacing between clay particles and promoting the partial exfoliation of nanoparticles in LPP/

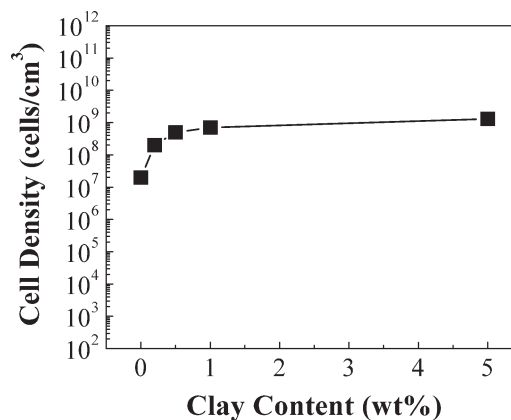


**Figure 9** Effect of clay content on foam cell density of LPP/clay nanocomposite foams at die temperature of 150°C.

clay nanocomposites during the foaming process of nanocomposites; (2) the addition of small amounts of clay particles to LPP during the foaming process suppresses the cell coalescence characteristic of LPP that exhibit low viscosities and weak melt strengths; (3) optimum clay content of 0.5–1 wt % can be used to prepare good LPP/clay nanocomposite foams that have a volume expansion ratio of around five and cell density of around  $10^9$  cells/cm<sup>3</sup>.

## References

1. Lee, S. T. *Foam Extrusion: Principles and Practice*; CRC: Lancaster, 2000.
2. Park, C. B.; Doroudiani, S.; Kortschot, M. T. *Polym Eng Sci* 1998, 38, 1205.
3. Naguib, H. E.; Park, C. B.; Reichelt, N. *J Appl Polym Sci* 2004, 91, 2661.
4. Naguib, H. E.; Park, C. B.; Panzer, U.; Reichelt, N. *Polym Eng Sci* 2002, 42, 1481.
5. Leaversuch, R. D. *Mod Plast* 1996, 73, 52.
6. Park, J. J.; Katz, L.; Gaylord, N. G. U.S. Pat. 5,116,881 (1992).
7. Bradley, M. B.; Phillips, E. M. *SPE ANTEC Tech Pap* 1990, 36, 717.
8. Park, C. B.; Cheung, L. K. *Polym Eng Sci* 1997, 37, 1.
9. Alexandre, M.; Dubois, P. *Mater Sci Eng, R* 2000, 28, 1.
10. Qi, Z. N.; Shang, W. Y. *Polymer/Layered Silicate Nanocomposites: Theory and Practice*; Chemical Industrial Publications: Beijing, 2002.
11. Giannelis, E. P. *Adv Mater* 1996, 8, 29.
12. Shah, D.; Maiti, P.; Gunn, E.; Schmidt, D. F.; Jiang, D. D.; Batt, C. A.; Giannelis, E. P. *Adv Mater* 2004, 16, 1173.
13. *Plastic Technology*. Available at: <http://www.ptonline.com/articles/200411fa2.html>; Accessed March 15, 2010.
14. Zeng, C. C.; Han, X. M.; Lee, L. J.; Koelling, K. W.; Tomasko, D. L. *Adv Mater* 2003, 15, 1743.
15. Lee, Y. H.; Wang, K. H.; Park, C. B.; Sain, M. *J Appl Polym Sci* 2007, 103, 2129.
16. Okamoto, M.; Nam, P. H.; Maiti, P.; Kotaka, T.; Nakayama, T.; Takada, M.; Ohshima, M.; Usuki, A.; Hasegawa, N.; Okamoto, H. *Nano Lett* 2001, 1, 503.
17. Pilla, S.; Kramschuster, A.; Gong, S.; Chandra, A.; Turng, L. S. *Int Polym Proc* 2007, 12, 418.
18. Yuan, M.; Winardi, A.; Gong, S.; Turng, L. S. *Polym Eng Sci* 2005, 45, 773.
19. Ramesh, N. S.; Rasmussen, D. H.; Campbell, G. A. *Polym Eng Sci* 1994, 34, 1685.
20. Ramesh, N. S.; Rasmussen, D. H.; Campbell, G. A. *Polym Eng Sci* 1994, 34, 1698.
21. Lee, J. W. S.; Wang, K. H.; Park, C. B. *Ind Eng Chem Res* 2005, 44, 92.
22. Zheng, W. G.; Lee, Y. H.; Park, C. B. *J Cell Plast* 2006, 42, 271.